THE DISTRIBUTION OF ALUMINUM-26 ABUNDANCES IN CAIS FROM CO3 CHONDRITES. A. T. Hertwig[1] and M.-C. Liu[1], [1] Department of Earth, Planetary, and Space Sciences, University of California, Los Angeles, CA 90095 (hertwig@ucla.edu).

Introduction: Ca-Al-rich inclusions (CAIs) are the oldest dateable solids in the Solar System [e.g., 1, 2] with an absolute radiometric Pb-Pb age of 4567.30 ±0.16 Ma [2]. Many large, cm-sized CAIs have been found to have initial $^{26}Al/^{27}Al$ ratios consistent with $5.2(\pm0.10)\times10^{-5}$ by both bulk-sample and in-situ measurements [e.g, 3, 4], but several are also characterized by $^{26}Al/^{27}Al$ lower than this value [e.g., 4]. Such variations in initial $^{26}Al/^{27}Al$ of CAIs and other refractory inclusions could be attributed to reheating of inclusions in the solar nebula following their initial formation or different formation events separated in time [e.g., 5-7]. Therefore, the distribution of initial $^{26}Al/^{27}Al$ can provide information about the timing of high-temperature events in the early stages of solar system's evolution.

In contrast to those in CV chondrites, refractory inclusions in CO chondrites are usually smaller (<500 µm, [8]) and mineralogically more pristine judging from the presence of early condensate phases predicted by equilibrium thermodynamics (e.g., corundum and hibonite, [e.g., 9]) and the often irregular shape of inclusions. Small (< 50 µm), fine-grained refractory inclusions are in particular interesting as they are messengers of initial dust formation and coagulation in the solar nebula, but determination of precise internal isochrons by secondary ion mass spectrometry (SIMS) has been often hindered by the small grain sizes of their constituents [7, and refs therein]. Recently, more advanced instrumentation [e.g., 10] has enabled a high-precision, high spatial resolution study of such small inclusions for $^{26}Al/^{27}Al$ by the internal isochron method [7], in which roughly two dozen refractory inclusions (30−100 µm in size) in the Allan Hills (ALH) A77307 (CO3.0) meteorite were analyzed. Two main populations of samples were revealed to have well-defined $^{26}Al/^{27}Al = 5.40(\pm0.13)\times10^{-5}$ and $4.89(\pm0.10)\times10^{-5}$. The former peak suggests a 50,000-year timescale between the condensation of µm-sized dust and initial coagulation, and the latter peak indicates the timing of nebula-wide thermal processing, ~0.1 Myr after condensation [7].

The work published in [7] is just the beginning of a comprehensive study of $^{26}Al/^{27}Al$ in small fine-grained CO3-chondrite CAIs. In order to improve the statistics on the ^{26}Al abundance distribution, we analyzed 12 more refractory inclusions from Yamato (Y)-81020 (CO3.05) (Fig. 1) and Dar al Gani (DaG) 005 and 027 (CO3) (Fig. 2). Preliminary data are presented here. Only one ^{26}Al study of a fine-grained inclusion from Y-81020 has been reported so far [11]. CAIs from DaG 005 and 027 have not been analyzed for Mg isotopes, but preliminary data on Ti isotopes have been reported for three of them [12]. Since Yamato CAIs are fine-grained and DaG CAIs are mostly coarse-grained, this study will also allow for a comparison of $^{26}Al/^{27}Al$ between these two types of inclusions from CO chondrites.

Methods: The Al-Mg systematics was analyzed in one thin section (Y-81020) and two epoxy-mounted thick sections (DaG 005/027) with the Cameca ims-1290 ion microprobe at UCLA [10] either by simultaneously collecting $^{24}Mg^+$, $^{25}Mg^+$, $^{26}Mg^+$ and $^{27}Al^+$ ions using multiple faraday cups (FCs) for spinel, hibonite, and melilite analyses [10, see for analytical detail] or by using the axial electron multiplier (EM) in mono-collection mode (only for melilite in Y-81020 CAIs). Beam sizes were approx. ~5 µm (1-3 nA, O_3^-) and 2 µm (~0.04 nA, O_3^-) for multi- and mono-collection analyses, respectively. Burma spinel, Madagascar hibonite and a melilite glass were used for characterizing the instrumental mass fractionation and relative sensitivity factor (RSF) for Al and Mg. For inclusions in Y-81020, prospective areas of analysis were marked using the Nova 600 SEM/FIB System (Ga beam) at UCLA, generally following descriptions in [13]. Data reduction mostly follows [10]. Isochron regression was done using [14]. Uncertainties on initial $^{26}Al/^{27}Al$ and $\delta^{26}Mg_0^*$ are at the 2s level.

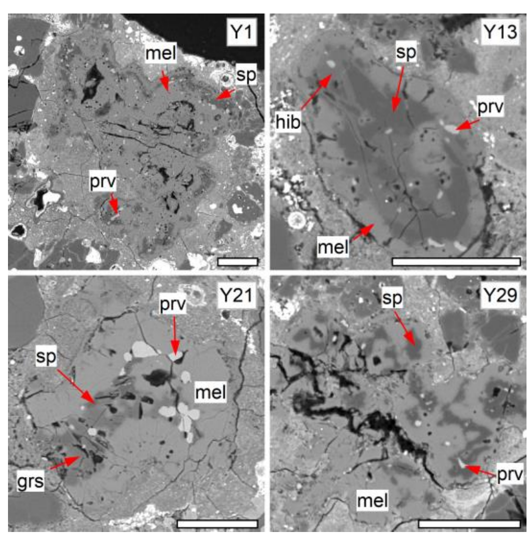

Fig. 1: BSE images of 4 of the 6 inclusions analyzed in Y-81020. Scale bar in all images is 50 µm.

Results: The analyzed inclusions in Y-81020 are 50-300 µm across and, except for Y13, irregularly shaped (Fig 1). All 6 inclusions contain spinel (sp), melilite (mel), and perovskite (prv); inclusion Y13 also contains hibonite (hib); Y21 grossite (grs). The analyzed coarse-grained CAIs in DaG 005 and 027 (mel-sp ±hib ±px) are up to 1 mm in size and show curved margins; most are fragments or have edges chipped off as indicated by discontinuous rims (Fig. 2).

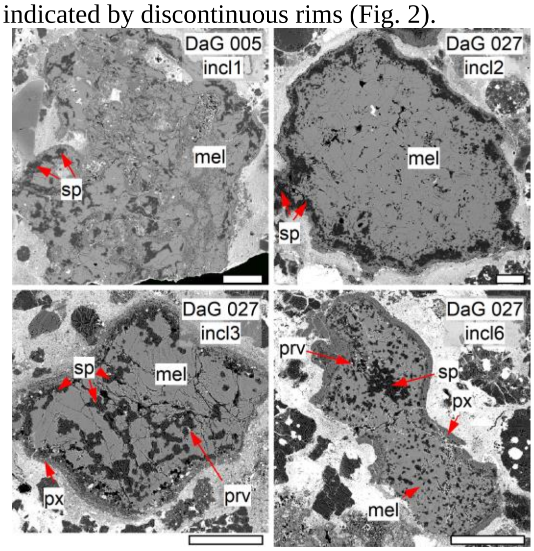

Fig. 2: BSE images of 4 of the 6 inclusions analyzed in the DaG 005 and DaG 027 chondrites. Scale bar in all images is 100 µm.

Initial $^{26}Al/^{27}Al$ for the six inclusions in Y-81020 range from 4.32(±0.40) $\times 10^{-5}$ to 5.16(±0.36) $\times 10^{-5}$. The $\delta^{26}Mg_0^*$ are indistinguishable from 0‰ within analytical uncertainty. Initial $^{26}Al/^{27}Al$ for the six coarse-grained inclusions in DaG 005 and 027 range from 3.57(±0.54) $\times 10^{-5}$ (not shown) to 4.65(±0.34) $\times 10^{-5}$. The $\delta^{26}Mg_0^*$ are variable and range from 5.14 ±4.24% to –0.10 ±0.12‰.

Discussion: With one exception, initial $^{26}Al/^{27}Al$ of the fine-grained CAIs measured in Y-81020 are consistent with 5.2 $\times 10^{-5}$. The initial $^{26}Al/^{27}Al$ of the only exception [Y21, 4.32(±0.40)$\times 10^{-5}$] is only marginally resolved from the second peak [4.89(±0.10)$\times 10^{-5}$] observed in the probability distribution of fine-grained inclusions from ALHA77307 [7] that corresponds to nebula-wide reprocessing of material.

In contrast, only one of the coarse-grained CAIs from the DaG chondrites (DaG 027 incl6) is within error consistent with 5.2 $\times 10^{-5}$. The range of observed initial $^{26}Al/^{27}Al$ of the other CAIs corresponds to a time span of ~0.25 Myrs and suggests thermal reprocessing of coarse-grained CAIs in DaG 005 and 027 ~0.4 Myrs after the onset of dust formation (5.4 $\times 10^{-5}$), when interpreted in the context of the scenario presented in [7]. Overall, the data is consistent with variations observed for formation ages of Vigarano CAIs [4].

Acknowledgments: We would like to thank G. Brennecka for providing the DaG 005 and 027 thick sections.

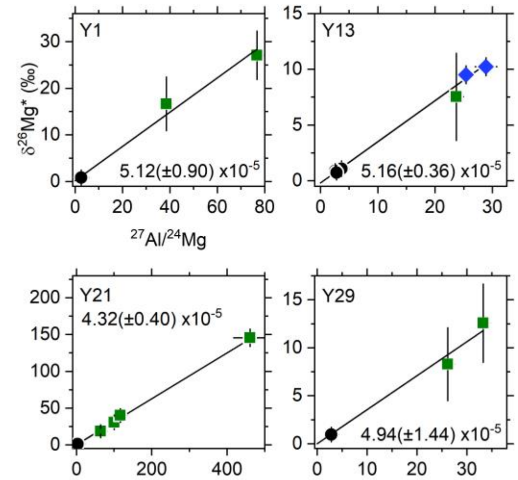

Fig. 3: Isochron diagrams of select inclusions in Y-81020. Circles: sp, square: mel, diamond: hib. Errors are 2s.

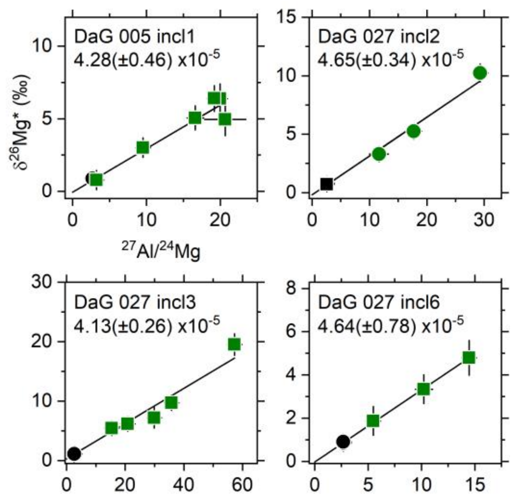

Fig. 4: Isochron diagrams of select inclusions in DaG 005 and 027. Errors and symbols as in Fig. 3

References: [1] MacPherson G. J. (2014) *In*: Treatise on Geochemistry. 139–179. [2] Connelly J. N. et al. (2012) *Science, 338*, 651–655. [3] Jacobsen B. et al. (2008) *Earth Planet. Sc. Lett., 272*, 353–364. [4] MacPherson G. J. et al. (2012) *Earth Planet. Sc. Lett., 331-332*, 43–54. [5] MacPherson G. J. and Davis A. M. (1993) *Geochim. Cosmochim. Acta, 57*, 231-243. [6] Kita N. T. et al. (2013) *Meteorit. Planet. Sci., 48*, 1383–1400. [7] Liu M.-C. et al. (2019) *Science advances, 5*, 1–8. [8] Russell S. S. et al. (1998) *Geochim. Cosmochim. Acta, 62*, 689–714. [9] Grossman L. (1972) *Geochim. Cosmochim. Acta, 36*, 597–619. [10] Liu M.-C. et al. (2018) *International Journal of Mass Spectrometry, 424*, 1–9. [11] Ushikubo T. et al. (2017) *Geochim. Cosmochim. Acta, 201*, 103–122. [12] Render J. et al. (2019) LPS L, Abstract #1526. [13] Nakashima D. et al. (2015) *Earth Planet. Sc. Lett., 410*, 54–61. [14] Trappitsch R. et al. (2018) *ApJ, 857*, L15.